Significance of a Two-Domain Structure in Subunits of Phycobiliproteins Revealed by the Normal Mode Analysis

Hiroto Kikuchi,* Hiroshi Wako,† Kei Yura,‡ Mitiko Go,‡ and Mamoru Mimuro§

*Department of Physics, Nippon Medical School, Kawasaki 211-0063; †School of Social Sciences, Waseda University, Tokyo 169-8050; ‡Division of Biological Science, Graduate School of Science, Nagoya University, Nagoya 464–8602; and §Department of Physics, Biology, and Informatics, Faculty of Science, Yamaguchi University, Yamaguchi 753-8512, Japan

ABSTRACT Phycobiliproteins are basic building blocks of phycobilisomes, a supra-molecular assembly for the light-capturing function of photosynthesis in cyanobacteria and red algae. One functional form of phycobiliproteins is a trimeric form consisting of three identical units having C_3 symmetry, with each unit composed of two kinds of subunits, the α-subunit and β-subunit. These subunits have similar chain folds and can be divided into either globin-like or X-Y helices domains. We studied the significance of this two-domain structure for their assembled structures and biological function (light-absorption) using a normal mode analysis to investigate dynamic aspects of their three-dimensional structures. We used C-phycocyanin (C-PC) as an example, and focused on the interactions between the two domains. The normal mode analysis was carried out for the following two cases: 1) the whole subunit, including the two domains; and 2) the globin-like domain alone. By comparing the dynamic properties, such as correlative movements between residues and the fluctuations of individual residues, we found that the X-Y helices domain plays an important role not only in the C_3 symmetry assemblies of the subunits in phycobiliproteins, but also in stabilizing the light absorption property by suppressing the fluctuation of the specific Asp residues near the chromophore. Interestingly, the conformation of the X-Y helices domain corresponds to that of a module in pyruvate phosphate dikinase (PPDK). The module in PPDK is involved in the interactions of two domains, just as the X-Y helices domain is involved in the interactions of two subunits. Finally, we discuss the mechanical construction of the C-PC subunits based on the normal mode analysis.

INTRODUCTION

Several kinds of symmetric structures of pigment-protein complexes are found in photosynthetic pigment systems. These include the C_3 symmetry of phycobiliproteins in cyanobacteria (Schirmer et al., 1986), C_3 symmetry of peridinin-chlorophyll a-protein in a dinoflagellate (Hoffman et al., 1996), C_8 symmetry of light harvesting complex (LH) II in the purple photosynthetic bacterium *Rhodospirillum molischianum* (Koepke et al., 1996), C_9 symmetry of LH II in the purple photosynthetic bacterium *Rhodopseudomonas acidophila* (McDermott et al., 1995), and possibly C_{16} symmetry of LH I in the purple photosynthetic bacterium *Rhodopseudomonas viridis* (Karrasch et al., 1995). It is likely that an increase in the optical cross-section is realized by a repeated structure comprised of a single building block, thereby leading to the symmetry structure of the antenna system.

Phycobiliproteins (PBPs) are major photosynthetic antenna pigments in cyanobacteria, red algae, and cryptomonad (Gantt, 1981; Bryant, 1991; Tandeau de Marsac, 1991; Grossman et al., 1993; Rüdiger, 1994; Sidler, 1994; Bald et al., 1996; Mimuro et al., 1999). The PBP monomer consists of one α-subunit and one β-subunit, while the trimer in C_3 symmetry is a basic building block (Fig. 1). Two trimers form a hexamer with the help of a linker polypeptide (Tandeau de Marsac and Choen-Bazire, 1977) that binds them, and the hexamer units assemble to form a phycobilisome (PBS), which is the supramolecular architecture on the surface of thylakoid membranes (Gantt and Conti, 1966).

The crystal structures of several kinds of PBPs have been reported. In 1985, C-phycocyanin (C-PC) was isolated from the cyanobacterium *Mastigocladus laminosus* and was crystallized. Its three-dimensional structure was resolved for the first time at a 3 Å resolution (Schirmer et al., 1985), and was later refined to a 1.66 Å resolution (Dürring et al., 1991). The crystal structure shows that the two subunits have an essentially similar fold and consist of two domains (Fig. 2). One is a globin-like domain, since it has a structure similar to a globin fold, which contains seven helices that were named according to the names for myoglobin (Schirmer et al., 1986). There are also two additional helices, known as the X and Y, which form the other domain and are referred to herein as the X-Y helices domain. The X and Y helices are a key structure in the trimer unit because they determine the hinge angle between the globin-like and the X-Y helices domains. The molecular structure of C-PC is common to at least six reported kinds of PBPs: allophycocyanin (APC, Brejc et al., 1995), phycoerythrocyanin (PEC, Dürring et al., 1990), B-phycoerythrin (B-PE, Ficner et al., 1992), b-phy-

Received for publication 12 July 1999 and in final form 12 June 2000.

Address reprint requests to Dr. Hiroto Kikuchi, Department of Physics, Nippon Medical School, 2-297-2 Kosugi-cho, Nakahara-ku, Kawasaki 211-0063, Japan. Tel.: +81-44-733-3518; Fax: +81-44-722-1231; E-mail: kikuchi@nms.ac.jp.

Present address: Department of Biochemistry, University of Washington, Box 357350, Seattle, WA 98185-7350; Tel.: +1-206-543-1788; Fax: +1-206-685-1792; E-mail: kikuchi@nms.ac.jp.

Abbreviation used: INDO-CI, intermediate neglect of differential overlap-configuration interaction.

0006-3495/00/09/1587/14 $2.00

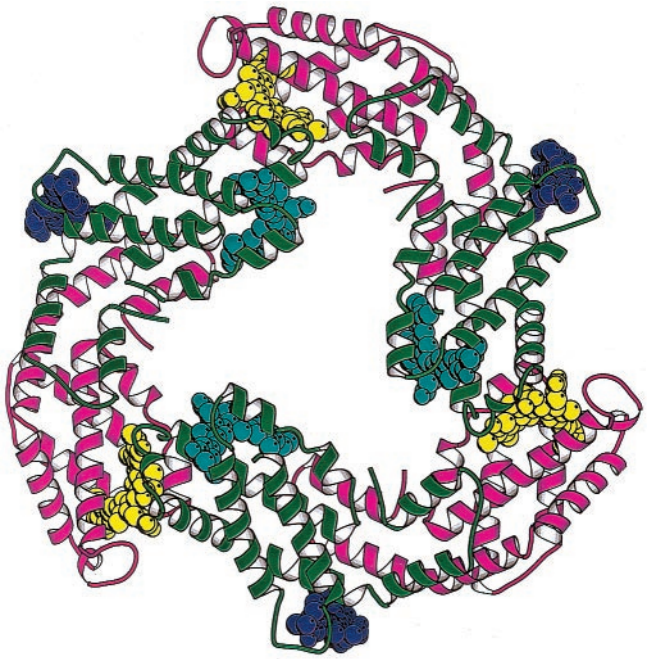

FIGURE 1 Three-dimensional structures of the trimeric $(\alpha\beta)_3$ C-phycocyanin isolated from *Fremyella diplosiphon* (PDB entry name, 1CPC) (Dürring et al., 1991. The α-subunit (*red*) and β-subunit (*green*) are shown by the ribbon model. Chromophores α84 (*yellow*), β84 (*blue*), and β155 (*dark blue*) are shown by the CPK model. The graphics in Figs. 1, 2, and 7 were made using the MOLSCRIPT program (Kraulis, 1991).

coerythrin (b-PE, Ficner and Huber, 1993), and R-phycoerythrin (R-PE, Chang et al., 1996). Recently, a structural analysis at 2.2 Å resolution was completed for APC with a linker complex (Reuter et al., 1999), and new structural data for R-PE have also been reported (Jiang et al., 1999; Ritter et al., 1999). Although the crystal structure of C-phycoerythrin is not yet known, its primary structure is highly homologous to other PBPs, which suggests that it may have a crystal structure similar to them. A high homology in the amino acid sequences (Fig. 3) and common crystal structures among PBPs clearly indicate that all PBPs are descendants of one common ancestral protein.

All PBPs have chromophores, which are derivatives of an open tetra-pyrrol ring. In the C-PC α-subunit, one chromophore, called α84, is covalently bound to Cys-84 through a thioether linkage with the vinyl substituent on the pyrrol ring A of the tetrapyrrole. The β-subunit has two chromophores, one binding to Cys-84 and the other to Cys-155 (Glazer, 1985, 1989), called β84 and β155, respectively. The seven kinds of PBPs mentioned above are classified by differences in chemical species of the chromophores, and their differences in molecular species and their interactions with the surrounding protein moiety result in different spectral properties. Interestingly, around all chromophores in PBPs there is an Asp residue at the position approximately equidistant from the nitrogen atoms on the B-ring and C-ring of the chromophore. By introducing a nitrogen atom carrying a formal π charge of $Z_C = +2$ instead of the pyridine-type nitrogen ($Z_C = +1$) on the C-ring, while leaving the number of π electrons in the chromophore unchanged, the red-shift of the visible absorption band can be reproduced successfully on the basis of the Pariser-Parr-Pople (π-electron) approximation (Pariser and Parr, 1953a, b; Pople, 1953) in C-PC (Scharnagl and Schneider, 1989). By using an INDO-CI program (Sakuranaga et al., 1979), the relationship between the protonation of the nitrogen atom on the C-ring of the chromophore and the optical properties of C-PC could be more precisely studied, including the oscillator strength. We have reported that the protonation of the nitrogen atom on the C-ring was a key to reproducing the observed red-shift of the absorption maximum and the oscillator strength (Kikuchi et al., 1997). Therefore, the Asp residue near the chromophore plays an important role in the light absorption function through protonation of the chromophore.

The present study investigated the significance of protein structures to biological function, particularly light absorption property of the chromophore. From a visual inspection of the three-dimensional structures of the C-PC trimer, it is obvious that the X-Y helices domain serves as the glue of the two subunits, and that the hinge angle between the globin-like and the X-Y helices domains is a key factor in the C_3 symmetric structure (Fig. 2). However, it is difficult to understand the mechanical and dynamical significance of the two-domain structure for the function of C-PC based on the static structure alone. Therefore, we adopted normal mode analyses using the following strategy: one analysis was applied to the whole α- or β-subunit in C-PC (i.e., including both domains), while the other was applied only to the globin-like domain, because the normal mode analysis can provide information on the interactions between amino acid residues that cannot be derived from the static structure alone. Using these analyses we investigated dynamic properties such as the correlative movements between residues and fluctuations of individual residues in the C-PC subunits. We found that the correlative movements of the globin-like domain of each subunit changed considerably when the X-Y helices domain was removed, and that the two-domain structure of the subunits functions to suppress the fluctuation of the above-mentioned Asp residues near the chromophore. On the basis of these results, we determined the potential significance of the X-Y helices domain to the whole structure and its optical properties and elucidated the functional significance of the mechanical constructions of the C-PC subunits.

MATERIALS AND METHODS

The crystal structure data for C-PC isolated from the cyanobacterium *Fremyella diplosiphon* (1CPC in PDB entry code; Dürring et al., 1991) resolved at a 1.66 Å resolution was adopted from the Protein Data Bank

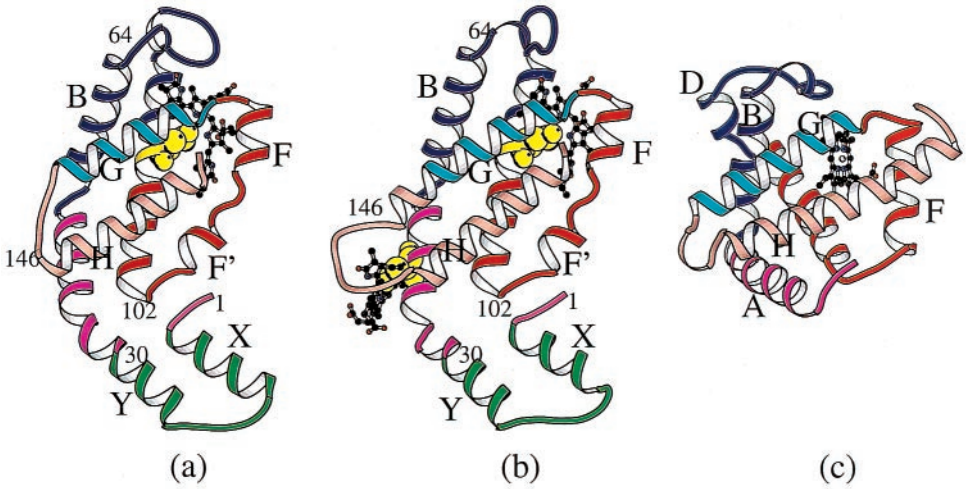

FIGURE 2 Three-dimensional structures of the α-subunit (*a*) and β-subunit (*b*) of C-phycocyanin from *F. diplosiphon* (Dürring et al., 1991), and that of myoglobin (*c*) from *Physeter catodon* (1MBD, Phillips, 1980). Asp-87 and Asp-39 are shown by the CPK model in yellow, and chromophores are shown by the ball-and-stick model in (*a*) and (*b*). Heme in (*c*) is also shown by the ball-and-stick model. The ribbons in (*a*) and (*b*) are colored according to the segments (S1–S8); S1, S2, S3, S4-S5, S6, S7, and S8 are represented by the colors magenta, green, magenta, dark blue, red, blue, and pink, respectively. In (*c*) the helices A, B–D, E–F, G, and H are represented by the colors magenta, dark blue, red, blue, and pink, respectively.

(PDB; Bernstein et al., 1977). The structural data for myoglobin (1MBD; Phillips, 1980) were used for a comparison. The ligand molecules, chromophores for C-PC, and the heme group for myoglobin were not included in the computation because this was the initial analysis of the dynamic structures of the subunits, and thus the interactions between protein and ligand(s) were reserved for later study.

For the calculation of the normal mode analysis we used the FEDER/2 computer program (second version, Wako et al., 1995; first version, Wako and Go, 1987), which adopts the potential functions of the program ECEPP developed by the Scheraga group (Momany et al., 1975; Nemethy et al., 1983). In this program, only dihedral angles were treated as independent variables, with the bond lengths and bond angles kept fixed. For the purpose of the calculation, the subunit was assumed to be in a vacuum.

Before carrying out the normal mode analysis, all x-ray data were refined geometrically and energetically in accord not only with the molecular model, but also with the conformational energy functions used in FEDER/2. In the refinement, the conformational energy of a given protein was minimized under the constraints for fitting the calculated conformation to the x-ray conformation (Wako, 1989a, b). The constraints were relaxed gradually. In the last stage of the refinement, only the conformational energy was minimized without the constraints. This minimization procedure could successfully lead the protein conformation to one of the local energy minima very close to the x-ray conformation. The second derivative matrices of the conformational energy function at the obtained minimum points had no negative eigenvalues for any proteins (Go et al., 1983), which is an inevitable condition to be satisfied in the normal mode analysis, that is, to have positive frequencies in all vibrational modes.

The time-averaged properties calculated in the normal mode analysis to explore the dynamic aspects of protein conformations have been discussed elsewhere (Go et al., 1983; Levitt et al., 1985; Nishikawa and Go, 1987; Wako, 1989a, b). In the present study we focused on the correlative movements of atoms. The correlation coefficient γ_{ij} between atoms i and j in their mutual movements is defined as

$$\gamma_{ij} = \frac{\langle \Delta r_i \cdot \Delta r_j \rangle}{\langle \Delta r_i^2 \rangle^{1/2} \langle \Delta r_j^2 \rangle^{1/2}}$$

where Δr_i and Δr_j are atomic displacement vectors from the minimum energy conformation for a given normal mode, and $\langle \cdots \rangle$ denotes an average over all the normal modes and time. We also calculated the root-mean-square (r.m.s.) displacement $\langle \Delta r_j^2 \rangle^{1/2}$ from the minimum energy conformation. The correlation coefficient (or the r.m.s. displacement) was calculated only for a C_α atom pair (or a C_α atom) as a representative of each residue pair (or each residue). The temperature was set to 300 K for all calculations.

The vibrational frequencies of the normal mode analyses of C-PC were in a range from 1.7 cm^{-1} to 969 cm^{-1} in the α-subunit and from 1.5 cm^{-1} to 1007 cm^{-1} in the β-subunit, which corresponded to 30 fs to 20 ps in the time region for both subunits.

RESULTS

Correlative movements in the α-subunit

Fig. 4 *A* shows the correlation coefficients of the C-PC α-subunit. The actual values of the correlation coefficient γ_{ij} between residues i and j in the map were in a range between -1 and 1, and those values are shown by five colors: when $0.4 < \gamma_{ij} < 1$ (strong positive correlation), coefficients are shown in red; when $0.15 < \gamma_{ij} < 0.4$ (positive correlation), in pink; when $-0.15 < \gamma_{ij} < 0.15$ (neutral), in white; when $-0.40 < \gamma_{ij} < -0.15$ (negative correlation), in light blue; and when $-1 < \gamma_{ij} < -0.4$ (strong negative correlation), in dark blue. The value 0.15 was selected to critically distinguish the dynamic aspect of the α-subunit from that of the globin-like domain alone, and the value 0.4 to critically express a strong correlation among approximately four successive amino acid residues in the α-helix, as shown by diagonal regions of the map. It should be noted that the numbering of the amino acid residues represents a compromise between the α- and β-subunits (see Fig. 3). The amino acid residues of 141–142 and 151–160 were missing in the α-subunit, while the amino

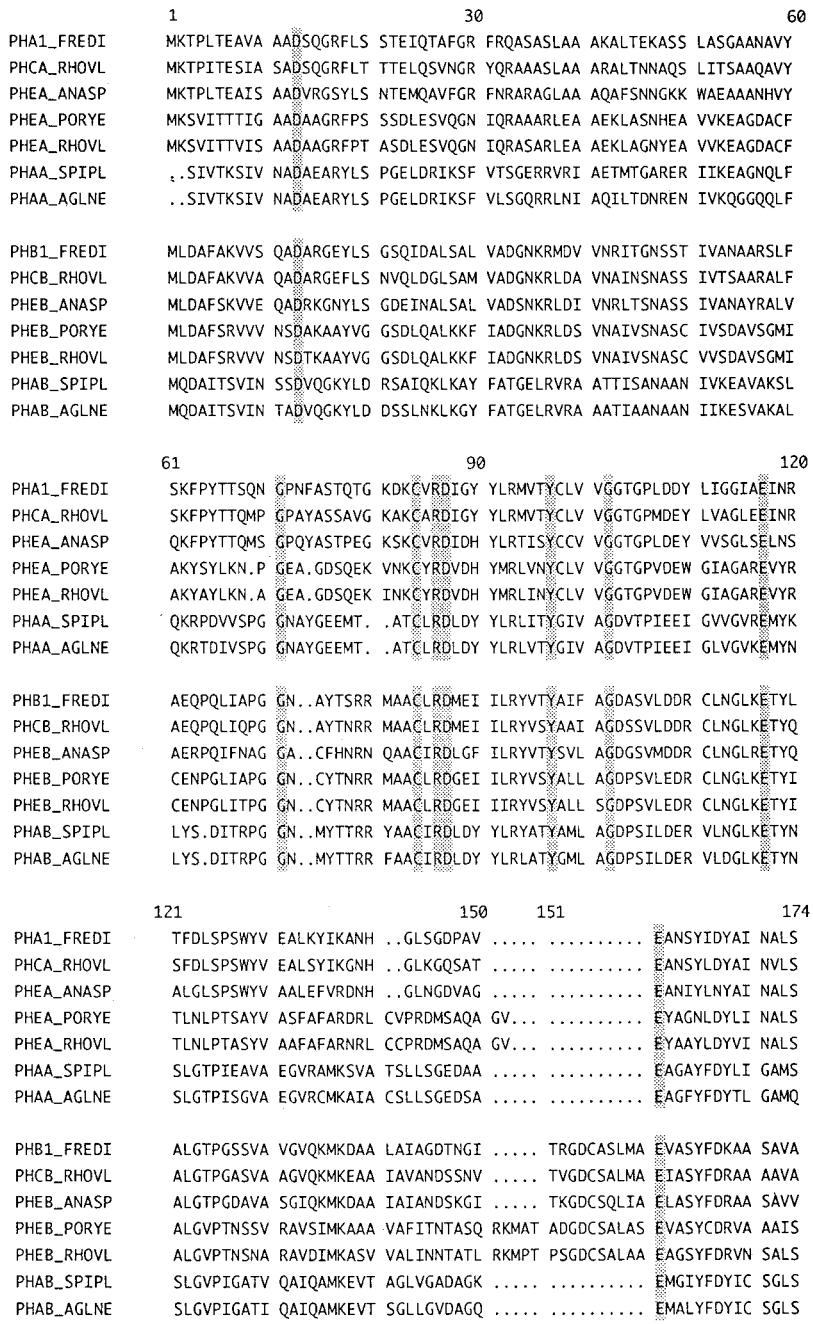

FIGURE 3 Multiple sequence alignment for the α- and β-chains of C-phycocyanin and its related proteins. The protein names are given by the SWISS-PROT entry codes. PHA1_FREDI, PHB1_FREDI: C-phycocyanin from *F. diplosiphon*; PHCA_RHOVL, PHCB_RHOVL: C-phycocyanin from *Rhodella violacea*; PHEA_ANASP, PHEB_ANASP: phycoerythrocyanin from *Anabaena* sp.; PHEA_PORYE, PHEB_PORYE: R-phycoerythrin from *Porphyra yezoensis*; PHEA_RHOVL, PHEB_RHOVL: B-phycoerythrin from *Rhodella violacea*; PHAA_SPIPL, PHAB_SPIPL: allophycocyanin from *Spirulina platensis*; and PHAA_AGLNE, PHAB_AGLNE: allophycocyanin from *Aglaothamnion neglectum*.

acid residues of 73–74 were missing in the β-subunit. The net numbers of residues of the α- and β-subunits were 162 and 172, respectively. The five colors in Fig. 4, *B–E*, 5, and 6 show the same classification of coefficients as in Fig. 4 *A*.

As shown by the first column of the correlation coefficients map (Fig. 4 *A*), the N-terminal amino acid of the α-subunit, methionine, showed a positive correlation with residues 1–7, 33–44, 90–115, and 147–173, and a negative correlation with the residues 9–25, 50–85, and 121–125. Any correlations with other residues were relatively neutral. By repeating the same procedures on every amino acid residue, we obtained the map consisting of clusters with the same signs in several regions. There were consecutive amino acid residues that have either positive or negative correlation coefficients to other consecutive amino acid residues, and are considered to behave as relatively rigid bodies. To analyze the dynamic structure between these consecutive amino acid residues, the idea of the segment that is different from helix is used in this paper. The segment was defined as consecutive amino acid residues that behave as relatively rigid bodies. In the case of the C-PC α-subunit, segments were classified on the basis of the

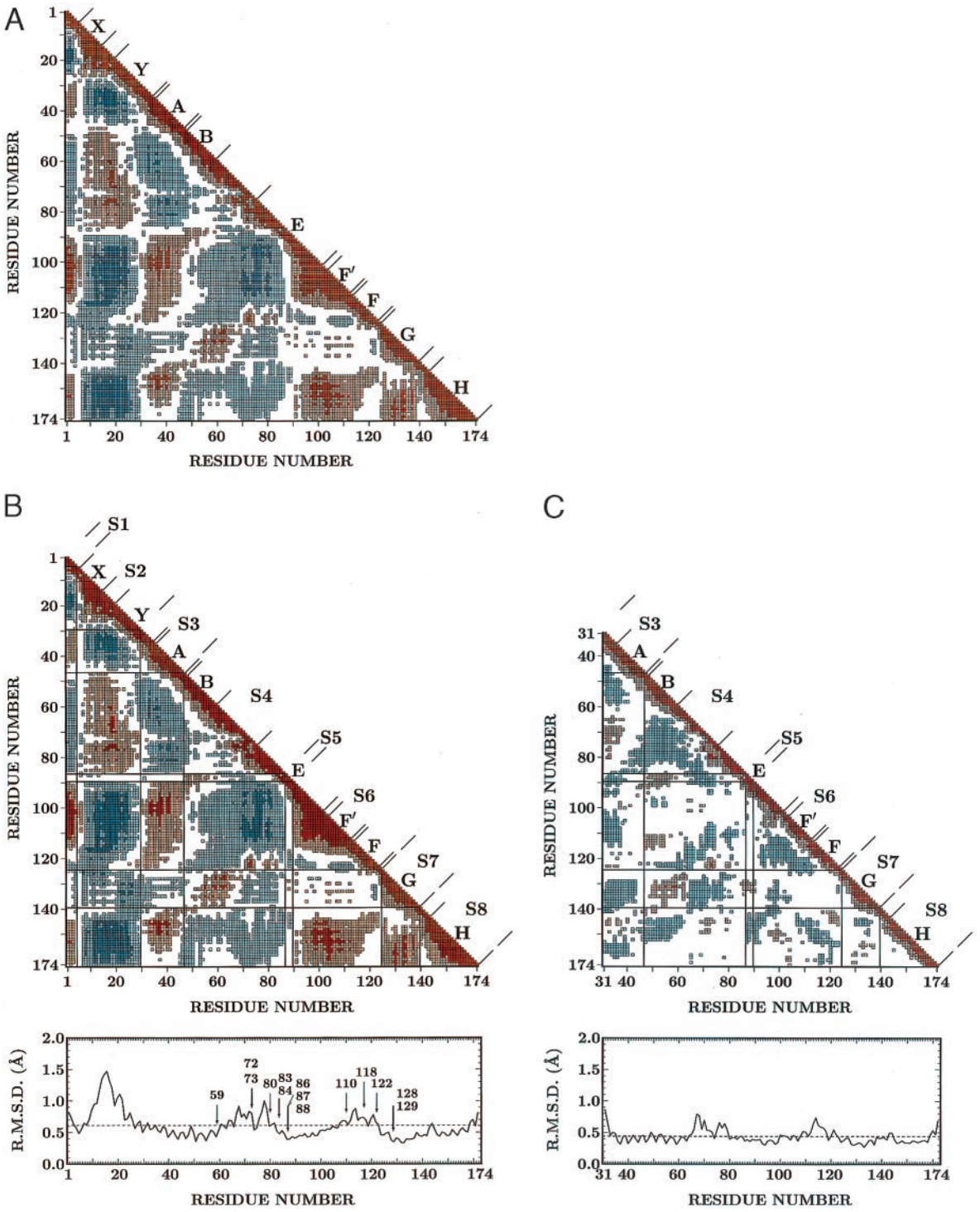

FIGURE 4 Correlation coefficient maps of C-phycocyanin. In (*A*), raw data for the correlation coefficients for the α-subunit were shown without a line to divide the regions. The correlation coefficients between residues were shown by different colors depending on their values (*upper triangle*) and root-mean-square displacements of residues (*lower box*) for the α-subunit (*B*), the globin-like domain of the α-subunit (*C*), the β-subunit (*D*), and the globin-like domain of the β-subunit (*E*). In the maps, amino acid residues fluctuating in the same direction, on average, are shown in red or pink, and those fluctuating in the opposite direction, on average, are shown in light blue or dark blue. A–E, F′, F, G, or H and S1–S8 on the diagonal line show locations of the respective helices and segments. Amino acid residues interacting with a chromophore are shown by arrows in the lower box.

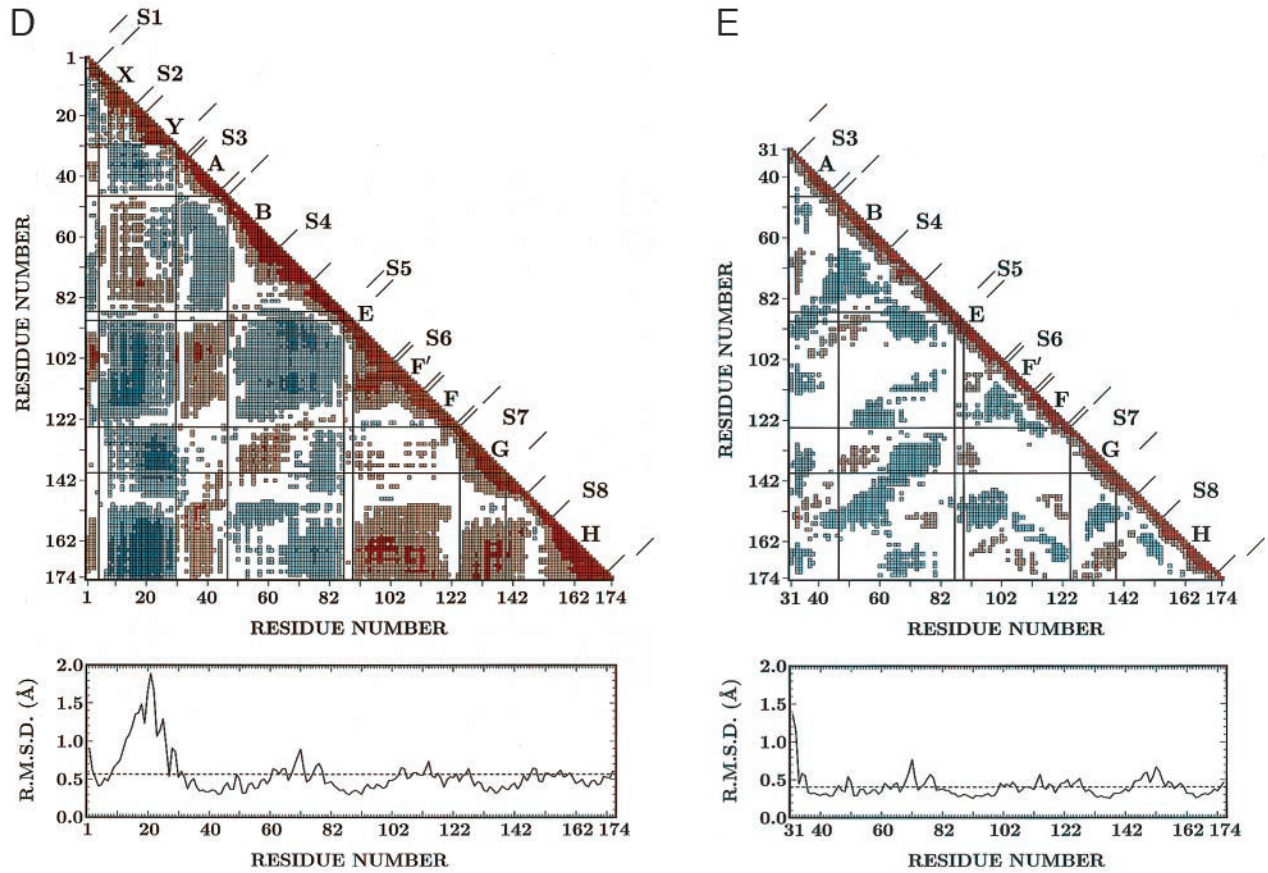

FIGURE 4 Continued.

following observations, and the segmentation patterns were shown by vertical and horizontal lines (Fig. 4 *B*). There was a clear boundary through which correlation factors changed from positive to negative, and vice versa: for example, between S1 and S2, S2 and S3, S3 and S4. Sometimes there were residues almost insensitive to the movement of other parts, and those were assigned to one segment, for example S5. Segments S6, S7, and S8 were classified on the basis of positive auto-correlation with themselves as shown by large positive triangles along the diagonal line. Based on these criteria, the whole sequence of the C-PC α-subunit was classified into eight segments, as shown by S1–S8: S1 (1–4), S2 (5–29), S3 (30–46), S4 (47–86), S5 (87–89), S6 (90–124), S7 (125–139), and S8 (140–174) (numbers in parentheses indicate the number of amino acid residues). Regions thus classified showed either positive or negative correlation with other regions, except for the cross-region between S4 and S7, and other several regions. The eight segments of the C-PC α-subunit might be divided into more ones. Namely, S4 (47–86) might also be divided into the two segments (47–70 and 71–86), or S6 (90–124), into the two segments (90–120 and 121–124). The boundaries of segments also showed ambiguity. Even though the concept of the segment was not general in the definition of the protein structure, these segments were nevertheless good indices when we compared the dynamic structures of several PBPs, such as the α-subunit (Fig. 4 *B*), the globin-like domain of the α-subunit (Fig. 4 *C*), the β-subunit (Fig. 4 *D*), the globin-like domain of the β-subunit (Fig. 4 *E*), and the α-subunit without the first four amino acid residues (Fig. 6).

Segment S5 was exceptionally short and was almost independent of the rest of the whole structure. One exception was the interaction with the B helix in S4. Segment S5 clearly divided the subunit into the two consecutive regions, $D_{seq}1$ (S1–S4) and $D_{seq}2$ (S6–S8), as shown in Fig. 4 *B*. In domain $D_{seq}1$, S2 (including helices X and Y) fluctuated in a positively correlated manner with S4 (consisting of the B helix, a loop connecting the B and E helices, and an N-terminal half of the E helix), while S1 and S3 (consisting mainly of the A helix) fluctuated in a negatively correlated manner with S2 and S4.

When we disregarded the chain connectivity, several new aspects were apparent. The correlation coefficients among S1, S3, S6, and S8 were positive, and were thus assigned to one large cluster located in the center of the α-subunit (Fig. 2 *a*). The correlative movements of S2 and S4 were also positive. However, S2 and S4 were spatially separated, locating at either side of the large center cluster. Segment S7

was positively correlated only with the B helix in S4, and these two segments were located close together. These results indicate that a normal mode analysis could elucidate the interactions due to spatial proximity (see Fig. 2 *a*). This allowed us to divide the subunit into three domains: $D_{sp}1$ (S1, S3, S6, S8), $D_{sp}2$ (S2), and $D_{sp}3$ (S4, S7). It should be noted that segment S1 belongs to $D_{sp}1$, but not to $D_{sp}2$. Segment S5 was assigned to a junction between domains $D_{sp}1$ and $D_{sp}3$. It may not be important whether or not the boundary between domains is strict, because ambiguity within one or two residues, if present, had no significant effect on the interpretation. It should be emphasized that domains $D_{seq}1$ and $D_{seq}2$, or $D_{sp}1$, $D_{sp}2$, and $D_{sp}3$, were classified according to the dynamic structure of the α-subunit on the basis of the normal mode analysis, while the globin-like and X-Y helices domains were classified according to the static structure.

Segment S5 (87–89) clearly divided the α-subunit into the two domains ($D_{seq}1$ and $D_{seq}2$) and its correlative movements with any other regions in the subunit were very few, except for those with the B helix in segment S4. The correlative movement between segment S5 and the B helix was due to the close position, but their interaction was relatively weak compared with the spatial relation. It should be noted that Asp-87 was located in segment S5, and that it was one of the main amino acids responsible for the optical property of the α84 chromophore due to interaction with two pyrrol rings of the chromophore (Kikuchi et al., 1997), which might be correlated with the relatively innocent dynamic structure of this region (see below).

Correlative movement in the C-PC α-subunit lacking the X-Y helices domain

As the second step in the analysis, we applied the normal mode analysis to the α-subunit lacking the X-Y helices domain, i.e., to the globin-like domain alone. As shown in the crystal structure (Fig. 2 *a*), the two domains are apparently independent of each other in a static sense. The correlation map of the subunit lacking the X-Y helices domain (Fig. 4 *C*) was completely different from that of the whole subunit (Fig. 4 *B*). We divided the globin-like domain into the same segments (Fig. 4 *C*) as those of the α-subunit to compare this domain with the α-subunit (Fig. 4 *B*). In general, areas of neutral movement increased, as represented by white areas. There were few residue pairs with positive correlation coefficients within the individual segments, i.e., S6, S7, and S8 (represented by red, blue, and pink in Fig. 2 *a*, respectively), and few regions with positive values between the two segments, as contrasted with the whole α-subunit. The pattern of the correlative movement of the α-subunit was completely modified due to lack of the X-Y helices domain. If the correlative movement shown in Fig. 4 *B* affects the biological functions, i.e., light absorption or energy transfer, the globin-like domain would not alone be responsible for these functions. In this context, the X-Y helices domain made the whole structure of the α-subunit fluctuate in a more concerted manner; they served to tune up the globin-like, chromophore-associating domain to show biological functions.

There was a rigid cluster in the globin-like domain; the B helix in S4 fluctuated in a positively correlated manner with S5 and with S7, irrespective of the presence or absence of X-Y helices (Fig. 4, *B* and *C*). These three regions were spatially close (Fig. 2), and assigned to a rigid cluster, which was a characteristic structure of a globin fold in the globin-like domain. In the α-subunit, this feature was not conspicuous due to the large correlation coefficients within each segment and between two segments, except for the rigid cluster. In the α-subunit without X-Y helices, the positive correlation between S5 and S7 became larger than that in the α-subunit, whereas a loss of X-Y helices induced a loose coupling within the globin-like domain as a whole.

As a comparison, we applied the normal mode analysis to myoglobin (Fig. 5), the entire structure of which is known to be similar to that of the globin-like domain of the C-PC subunits (Schirmer et al., 1985). Neutral regions were relatively abundant, as in the case of the α-subunit without the X-Y helices. The correlative movements between consecutive residues, including the feature of the rigid cluster in myoglobin, were observed in many regions, as in the case of the globin-like domain without the X-Y helices domain (Figs. 4 *C* and 5). However, we found two important differences between the α-subunit without X-Y helices (Fig. 4 *C*) and myoglobin (Fig. 5). One is the rigid cluster consisting of the B helix in S4, and of S5 and S7 in myoglobin; there was no positive correlation between the E helix and

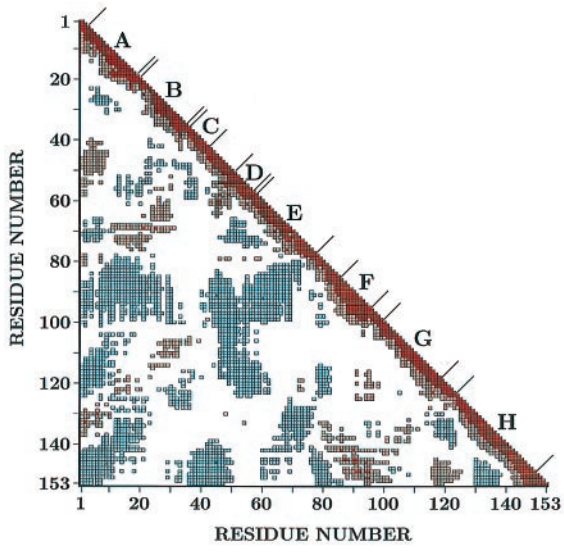

FIGURE 5 A correlation coefficient map for myoglobin. A–H on the diagonal line show locations of the respective helices (1MBD, Phillips, 1980). The colors depending on the coefficient values and notation in the map are the same as those in Fig. 4.

the G helix, even though other features of the rigid cluster were found. This feature was rather similar to the α-subunit. The other difference was the negative correlation between the E helix and the F helix in myoglobin (Fig. 5); these two helices were not in parallel, but rather were bound in a V-shaped configuration. These features reflected differences in the static structures of the two kinds of globin folds (see Discussion). Therefore, it was understood that the normal mode analysis could represent the following features. Even though the two proteins were similar to each other in terms of their three-dimensional structures, the difference in the interactions between the amino acid residues corresponding to common regions in structures was discriminated, as shown in the α-subunit and globin-like domain of the α-subunit. Conversely, even though the three-dimensional structures of the two proteins were not homologous, as in the case of myoglobin and the α-subunit of C-PC, the common feature of the interactions could be determined.

Fluctuations of individual residues around the minimum conformation

The normal mode analysis provides information about the fluctuations of the Cα atoms (i.e., residues) around the minimum energy conformation. The r.m.s. displacements of residues of the C-PC α-subunit and α-subunit without X-Y helices are shown in the lower boxes in Fig. 4, *B* and *C*, respectively. The horizontal broken line indicates a mean value of displacement. In the α-subunit, through a comparison with the mean value (0.61 Å), we found several regions showing relatively large fluctuations, such as residues 9–25, 67–79, and 112–121, as well as other regions showing relatively small fluctuations, such as 40–59, 83–101, and 125–137 (Fig. 4 *B*). The latter three regions corresponded to the B helix, the C-terminal half of the E helix, and the G helix, which were spatially close and thus fluctuated in a positively correlated manner. This supports the notion that these helices form a rigid cluster in the α-subunit.

The minimum of the fluctuation was observed at position 87 (Asp-87) on the E helix, which corresponded to the break point in the dynamic structure discussed above (S5 region). Furthermore, the carboxylate oxygen of Asp-87 was assigned to interact with the nitrogen atoms of pyrrol rings (the B- and C-rings of the chromophore, an open-tetra pyrrol ring), which brought both into a protonated state. In the neutral chromophore, the oscillator strength of the S_0-S_1 transition was very small (Kikuchi et al., 1997). The protonation of the nitrogen atom on the C-ring was critical in the optical functioning of the chromophore, especially for light absorption. We postulated that this minimum of the fluctuation of Asp-87 led to an increase in the stability of the electronic state of the protonated chromophore.

However, when the X-Y helices were missing from the globin-like domain, the average value of the fluctuation decreased (0.47 Å) due to lack of a largely fluctuating region, i.e., the X-Y helices. However, the local minimum point of the fluctuation was no longer observed (Fig. 4 *B* vs. Fig. 4 *C*). When we compared the values of the fluctuation of Asp-87, we found them to be the same in both cases. This indicates that the fluctuation, except for that of Asp-87, increases when the X-Y helices domain attaches to the globin-like domain, and that the fluctuation of Asp-87 does not increase even though the X-Y helices attach to the globin-like domain. This clearly indicated that the X-Y helices domain has a strong influence not only on the whole structure of C-PC, but also on its biological functions, such as light absorption. In order to utilize phycobilins as antenna pigment in proteins, a tight configuration of the chromophore is required, thus an interaction of Asp-87 with two pyrrol rings of the chromophores and the minimum fluctuation of Asp-87 are required for its functions. We concluded that the protein structure controls the optical properties of the chromophore through the X-Y helices, Asp-87, and the protonation of the nitrogen atom on the C-ring of the chromophore.

The amino acid residues 59, 72, 73, 80, 83, 84, 86, 87, 88, 110, 118, 122, 128, and 129 had at least one atom within 3 Å of the α84. The locations of these amino acids are indicated by arrows in the lower boxes in Fig. 4 *B*. Among these, Cys-84 is covalently bound to a chromophore, Arg-86 forms a hydrogen bond to a propionic acid, and Asp-87 interacts with the B- and C-rings of the chromophore. The fluctuations of most of the above 14 amino acid residues tended to show local minima. This supports the notion that the protein structure controls the stability of the chromophore. In the present study, the chromophore was not included in the calculation; however, if the chromophore is taken into consideration in this normal mode analysis, these features would be significantly enhanced due to stronger interactions between the amino acid residues and the chromophore (see Discussion).

Correlative movements in the C-PC β-subunit

The normal mode analysis was also applied to the β-subunit of C-PC. There are two chromophores in this subunit, β84 and β155, which are bound to Cys-84 and Cys-155, respectively, while the α-subunit has only one chromophore (α84). In the β-subunit, the amino acids that cause the protonation of the C-ring nitrogen atoms are Asp-87 and Asp-39 for β84 and β155, respectively. The insertion of the segment having 10 residues in the β-subunit, i.e., 151–160, including Cys-155, was particularly interesting.

The overall pattern of the correlation coefficient maps of the β-subunit (Fig. 4 *D*) was very similar to that of the α-subunit (Fig. 4 *B*). The segmentation and assignment of the domain structure on the basis of the dynamic structure for the α-subunit were essentially maintained in the β-subunit. In order to compare with the α-subunit we divided the

β-subunit into the same number of segments as we did the α-subunit: S1 (1–4), S2 (5–29), S3 (30–46), S4 (47–86), S5 (87–89), S6 (90–124), S7 (125–139), and S8 (140–174). In fact, the border behavior of S7 and S8 of the β-subunit was different from that of the α-subunit due to the insertion of 151–160. The segments S6 (*red* in Fig. 2 *a*), S7 (*blue*), and S8 (*pink*) contained many residue pairs with large positive correlation coefficients within each segment. Segment S5 was exceptionally short and was almost independent of the others; it clearly divided the subunit into the two consecutive regions, $D_{seq}1$ (S1–S4) and $D_{seq}2$ (S6–S8). In the domain $D_{seq}1$, segment S2 (including helices X and Y) fluctuated in a positively correlated manner with S4 (consisting of the B helix, a loop connecting the B and E helices, and an N-terminal half of the E helix), while S3 (consisting mainly of the A helix) fluctuated in a negatively correlated manner with S2 and S4. The analysis also allowed classification of the domains for the β-subunit based on their spatial proximity ($D_{sp}1$, $D_{sp}2$, $D_{sp}3$).

The pattern of correlative movement of the β-subunit without the X-Y helices (Fig. 4 *E*) was essentially similar to that of the α-subunit without the X-Y helices (Fig. 4 *C*). A rigid cluster was also found in the β-subunit without the X-Y helices (Fig. 4 *E*), i.e., the three regions, S5, S7, and the B helix in S4 were in close contact with each other (Fig. 2). Interaction between S5 and S7, however, was decreased in the β-subunit (Fig. 4 *D*), as was the case with the α-subunit (Fig. 4, *A* and *B*). A rigid cluster was thus assigned to a common structural feature to myoglobin, or C-PC subunits without the X-Y helices. This rigid cluster was maintained in the C-PC α-subunit and β-subunit with decreased interaction.

It should be emphasized that insertion of 10 amino acid residues (151–160) induced significant changes in the characteristics of the β-subunit. One of these changes was the presence of a neutral region; the three amino acid residues, 147, 148, and 149, looked like a new segment that was nearly independent of the others. The other change was differences in the correlative movements of residue pairs between S3 (30–46) and S7 (125–139); in the α-subunit, the correlation coefficients between these two were mainly negative, while they were not negative in the β-subunit. Changes in the property of S3 due to the insertion were clearly shown in the fluctuation of the amino acid residues (Fig. 4 *D*, *lower section*). A fluctuation around residues 38–42 was considerably suppressed compared with that in the α-subunit (Fig. 4 *B*, *lower section*), in addition to the 87th position. The 39th residue in the β-subunit was Asp, which directly interacts with the second chromophore of the β-subunit (β155) binding to the inserted Cys-155 (Fig. 3). The functional importance of Asp-39 for β155 was the same as that of Asp-87 for α84 or β84. In this sense, a structural modification due to the insertion caused a decrease in the fluctuation around the 39th residue, which induced the binding of an additional chromophore.

The role of the N-terminal part of the subunits

When the X-Y helices were attached to the globin-like domain, the fluctuation of the subsequent four segments showed a strong positive correlation with each other: in the case of the α-subunit, S1 (1–4) (the N-terminus), S3 (30–46) (the C-terminal region of the Y helix and the A helix), S6 (90–124) (the C-terminal half of the E, F′, and F helices), and S8 (140–174) (the H helix). These segments were assigned to $D_{sp}1$, and were closely located in the subunit (see Fig. 2 *a*). Of these four segments, only S1 was located outside of the globin-like domain. Therefore, it is reasonable to assume that even a small number of residues (i.e., four residues in S1) contributes significantly to the dynamic structure through a strong interaction with some regions in the globin-like domain.

In order to confirm this hypothesis we carried out the normal mode analysis for the C-PC α-subunit lacking four amino acid residues from the N-terminus. Fig. 6 shows the resulting correlation coefficient map. The number of residue pairs with strong positive correlation coefficients among S3, S6, and S8 in the whole subunit were markedly fewer in the subunit lacking the four residues (Fig. 4 *B*). This indicates that even only four amino acid residues in the N-terminus can strongly affect the dynamic structures of the whole protein. Because S1 was spatially close to the F′ and H helices (Fig. 2), the correlative movements of S1 with S6 containing the F′ helix, and of S1 with S8 containing the H helix, could be understood. It should be also pointed out that the loop between the E and F helices showed a strong positive correlation with the S7 (the G helix) (Fig. 6) when

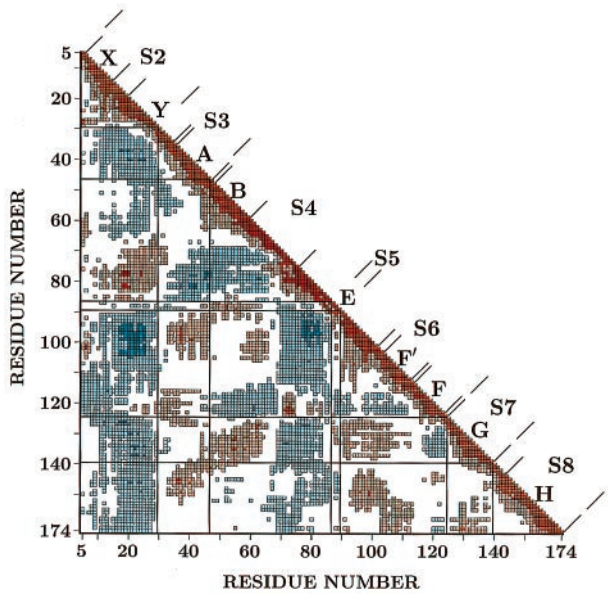

FIGURE 6 A correlation coefficient map for the α-subunit of C-phycocyanin from which the first four residues were removed. The colors depending on the coefficient values, notation for the helix, and segment are the same as those in Fig. 4.

the F′ helix lost the interaction with S1. Because this loop was spatially distant from S7 (the G helix), this correlative fluctuation could be realized through the interactions with the H helix that were in close contact with both the loop and the F′ helix. The N-terminal residues 1–4 thus appear to control the interaction between S5 and S7 (the G helix), and consequently contributed to the observed minimum fluctuation of Asp-87.

Fig. 6 clearly shows the presence of the rigid cluster assigned to the globin fold. The pattern of correlation coefficients was very similar to that of the α- or β-subunit without X-Y helices (Fig. 4, *C* or *E*) compared with that of the α- or β-subunit (Fig. 4, *B* or *D*): the correlated movement between S5 and S7 was stronger than that in the α- or β-subunit. This indicated that a loss of interaction between the X-Y helices and the globin-like domain induced an inherent stabilization of the globin-like domain and, further, that an interaction among S1, S6, and S8 is a determinative factor for the subunits of C-PC. This dynamic structure led to the observed minimum of the fluctuation of Asp-87, and this mechanical construction appears to be a critical factor for the optical properties of the chromophore, especially the light absorption function of this protein.

DISCUSSION

Dynamic structure of C-PC as revealed by the normal mode analysis

The present study is the first reported application of the normal mode analysis to the antenna proteins of photosynthesis. We introduced the concept of segments based on the dynamic structure. Investigation of the dynamic structure of C-PC yielded a very different view from that based on the static structure alone. The dynamic structure of the α-subunit was very different from that of the globin-like domain, the α-subunit without the X-Y helices domain. Our findings indicated that the X-Y helices domain plays an important role in the function of the optical properties of chromophores as well as in the structures comprising the monomer. We also identified a rigid cluster as an important feature of the globin fold. When the X-Y helices domain interacted with the globin-like domain through S1 and the loop between the E and F′ helices, the interaction between S5 and S7 (the G helix) making the rigid cluster was controlled through S8 (the H helix). The balance of these interactions caused the minimum of the fluctuation to be observed at Asp-87. Thus, the key regions of structural and functional significance were assigned to the following three factors: 1) an interaction between the S1 (the N-terminal region of the X-Y helices domain) and the loop connecting the E and F′ helices, 2) S8 (the H helix), and 3) the angle determined by the loop connecting the Y and A helices.

In the loop between the E and F′ helices, one residue, Gly-102, is well conserved in all the PBPs sequenced to date (Fig. 3). This residue directly interacted with the N-terminal of the subunit, and was responsible for the interaction between the X-Y helices domain and the globin-like domain. Furthermore, the hydrophobic residues (Y91, L92, V95, L107, I136, A162, Y165, and I166) around this interacting region were also well conserved, and formed a hydrophobic core within both subunits. This core structure may be involved in determining the angle between the two static domains. In addition, residues at L5 and F31, and those at L38, M94, Y97, and V100 interacted with the hydrophobic residues in the β-subunit (Figs. 3 and 7). The connecting region between the Y and A helices, i.e., between the X-Y helices and the globin-like domains, was critical for the interaction between the two subunits. It is only when the interactions within these hydrophobic regions are maintained that the hinge angle determined by the Y and A helices can be kept to ~120°. Clearly, the X-Y helices domain and the hinge angle must be considered important determinants for the function of phycobiliproteins because they affect the structure of their basic building blocks.

The normal mode analysis gave rise to a new aspect in the domain structure. In a static sense, the α- and β-subunits of C-PC consist of the two domains referred to as the globin-

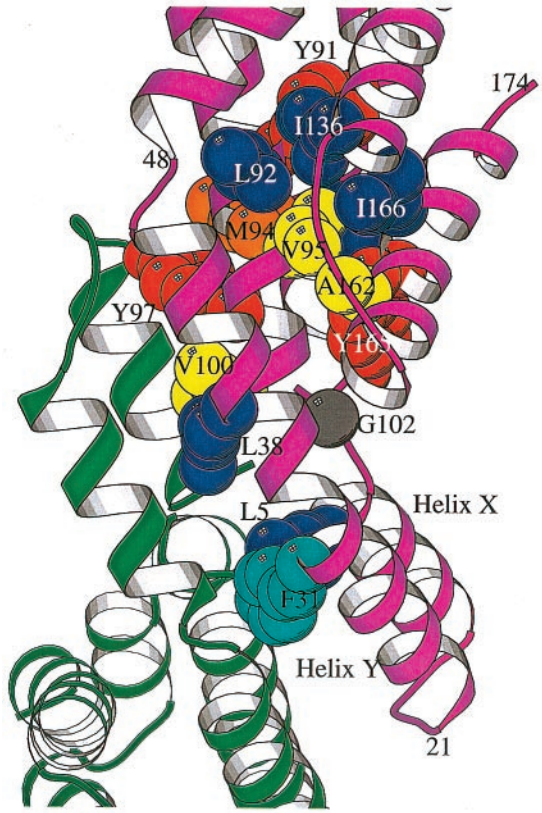

FIGURE 7 A hydrophobic core around the junction region between the globin-like and X-Y helices domain of C-phycocyanin. The hydrophobic residues in the α-chain (*magenta ribbon*) are shown by the CPK model. The β-chain is shown by the green ribbon only.

like and X-Y helices domains. However, the analysis revealed different domain structures, such as two-domain (i.e., $D_{seq}1$ and $D_{seq}2$) or three-domain (i.e., $D_{sp}1$, $D_{sp}2$, and $D_{sp}3$) structures in a dynamic sense. Irrespective of the definition of either domain structure in the dynamic sense, Asp-87 was shown to be a key residue for the dynamic structures of both subunits. In the β-subunit, insertion of the segment 151–160 suppressed the fluctuation of Asp-39. Asp-39 in the β-subunit alone and Asp-87 in both subunits are known to play an important role in the electronic state of the chromophore through protonation of the nitrogen atom on the C-ring of the chromophore (Scharnagl and Schneider, 1989; Kikuchi et al., 1997). It would be very difficult to determine these aspects from an analysis of the static structure alone.

The normal mode analysis also yielded a new perspective on the difference in the globin-fold between C-PC and myoglobin. Although the rigid cluster consisting of three segments was common between the two proteins, in C-PC the interaction between S5 and S7, and between the C-terminal part of the E and F′ helices, depended on the presence of the X-Y helices. In myoglobin, by contrast, there was no correlation between the N-terminal half of the E helix and the G helix (Fig. 5). This may be due to differences in the structures of the two (E and G) helices, i.e., the distance between the two helices was longer in myoglobin than in the C-PC subunits due to the more globular structure of myoglobin. Similarly, the interaction between the N-terminal part of the E helix and the F helix was less in myoglobin (Fig. 5) compared with that in the C-PC subunits (Fig. 4, *A* and *C*). This may be due to the steric effect of the two helices, i.e., in myoglobin they were connected in a V-shape, while they were parallel in the C-PC subunits. These results indicated that the correlative movements between the residues revealed by the normal mode analysis could reflect an inherent property (the rigid cluster) in the globin fold, and could also show the difference between the globin-like domain with and without the X-Y helices domain as well as the difference in the static structure in two kinds of globin folds.

A given border of segments classified by the normal mode analysis was not necessarily consistent with a given border of helices classified by the static structure in C-PC (Fig. 4, *A* and *C*). In some cases, the terminating point of a segment was in the middle of the helix, i.e., S2 versus the Y helix, or S5 versus the E helix. However, some segments corresponded to a particular helix, i.e., S7 versus the G helix, and S8 versus the H helix. Furthermore, one segment consisted of more than one helix and another component, i.e., S4 and S6. Because the concept of a segment included spatial proximity and correlative movement, it could differ from the structural continuity of a specific secondary structure (helix).

Origin of the X-Y helices

A globin fold is decomposable into four modules (Go, 1981). A module, defined as a compact structure within a globular domain, has on average ~15 contiguous amino acid residues (Go, 1983). A module boundary is identified by locating a local minimum of the centripetal profile, which is a profile of the average square C_α-C_α distances of a certain length of the segment against residue numbers (Go and Nosaka, 1987; Noguti et al., 1993). The correlation of the module organization of a protein with the exon/intron structure of the gene suggests that a module is an evolutionary unit of shuffling (Go and Noguti, 1995; Sato et al., 1999). The three-dimensional structure of C-PC suggests that the protein originated from a combination of the globin-like domain and the X-Y helices domain. The X-Y helices domain of the C-PC α-subunit corresponds to a single module (residues 1–28, Fig. 8 *a*) and that of the C-PC β-subunit is decomposable into two modules (residues 1–8 and 9–28, Fig. 8 *b*). The difference might be due to an additional chromophore β155 with which the X-Y helices domain of the α-subunit is in contact (Fig. 1). A slight distortion of the backbone structure, seemingly caused by the molecule, resulted in the observed difference. We used the module structure of the α-subunit for our analysis. Module M1 of the α-subunit plays an important role in the C_3 symmetry assemblies and in inducing a concerted fluctuation elsewhere in the C-PC. The correspondence of the X-Y helices domain to the module indicates that C-PC acquired module M1 of the α-subunit by adding a DNA base sequence encoding module M1 of the subunit to the 5′ of the gene that encoded a prototype of C-PC, namely the globin-like domain. This scenario implies that a similar module to M1 of the α-subunit will be found in different proteins. We searched the Protein Data Bank (Bernstein et al., 1977) for a structurally similar module to M1 of the α-subunit and found module M4 in pyruvate phosphate dikinase (PPDK, Fig. 8 *c*), a histidyl multiphosphotransfer enzyme that synthesizes adenosine triphosphate (Herzberg et al., 1996), which is a protein apparently unrelated to C-PC. The similarity in the amino acid sequences and the three-dimensional structures of the modules suggests that module M4 of PPDK may play a similar role to module M1 in the C-PC α-subunit (Fig. 8). In C-PC, the α-subunit module M1 is an interface of the α- and β-subunits. A portion of the β-subunit and the chromophore β155 are in contact on the C-terminal side of module M1. Module M4 in PPDK is located in an ATP-binding domain and interacts with a four-helix bundle domain in PPDK. A portion of the four-helix bundle domain is in contact on the C-terminal side of module M4 of PPDK. As shown in Fig. 8, the contact surface of module M4 with the four-helix bundle domain in PPDK and that of module M1 of the C-PC α-subunit with the β-subunit are both located on the distant side of the C-terminal helix.

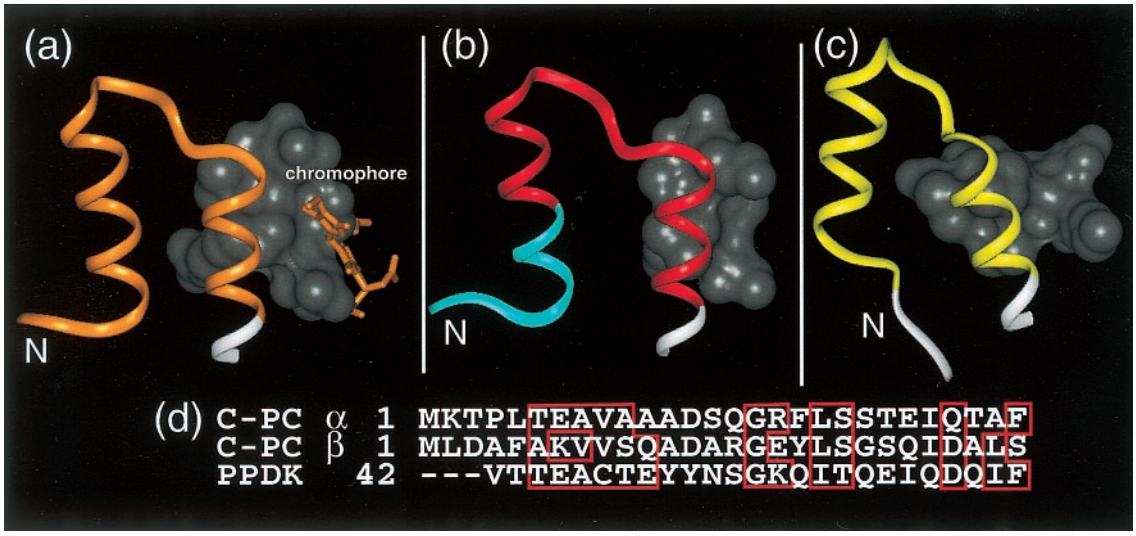

FIGURE 8 Similar modules in C-PC and pyruvate phosphate dikinase (PPDK) in C_α trace model. (*a*) The three-dimensional structure of module M1 that corresponds to the X-Y helices domain of the C-PC α-subunit. Module M1 is from residues 1–28. The white section represents the residues belonging to the next module. The chromophore molecule β155 lies at the interface of the α- and β-subunits. A portion of the β-subunit in contact with module M1 of the α-subunit is shown in dark gray. (*b*) Modules of the C-PC β-subunit corresponding to module M1 of the α-subunit. The blue region represents module M1 and the red region represents module M2. The difference in the number of modules in the α- and β-subunits might be caused by the different interactions at the subunit interfaces. Module M2 in the β-subunit is not in contact with a chromophore molecule, but is an interface of the α- and β-subunits. The portion of the α-subunit in contact with module M2 in the β-subunit is shown in dark gray. (*c*) Module M4 in PPDK having a similar three-dimensional structure to module M1 of the C-PC α-subunit and M1 + M2 of the C-PC β-subunit. Module M4 starts with residue 41 and ends at residue 66. The module is an interface between the ATP-binding domain where the module locates and a four-helix bundle domain. The portion of the domain in contact with module M4 is shown in dark gray. (*d*) Alignment of the amino acid sequences of module M1 of the C-PC α-subunit, modules M1 + M2 of the C-PC β-subunit, and module M4 of PPDK based on superposition of the three-dimensional structures. Root-mean-square deviations of Cα atoms are 2.0 Å for the pair of module M1 of the C-PC α-subunit and module M4 of PPDK, and modules M1 + M2 of the C-PC β-subunit and module M4 of PPDK. The residues with similar characteristics between module M1 of the C-PC α-subunit and module M4 of PPDK, and between modules M1 + M2 of the C-PC β-subunit and module M4 of PPDK, are boxed.

Effect of the chromophore on the structure

In the present study we did not include in our calculations the ligand molecules, the chromophores for C-PC, or a heme group for myoglobin because we sought to first clarify the nature of the peptides. Only after obtaining those data did we consider introducing interactions between peptide moieties and chromophores to learn more about the changes brought about by these interactions. In our calculations, the chromophore space was replaced with a vacuum. However, the energy minimum conformation of the peptide without the chromophore was very close to the x-ray conformation because the FEDER/2 program was developed to satisfy the above condition for a given calculation method (Wako, 1989a,b). Accordingly, even though there are no interactions between the chromophore and the amino acids surrounding it, interactions between the amino acids surrounding the chromophore were expected to be almost the same as those in the case where the chromophore had been included. Therefore, even under this condition, a certain, albeit imperfect, degree of interaction between the chromophore and its surrounding moieties was included in the calculation. Thus, we assumed that the presence of the chromophore would induce smaller fluctuations of the amino acid residues around the chromophore due to the interactions between the chromophore and its surrounding moiety. Of course, the interaction between the chromophore and Asp-87 is one of the above-mentioned interactions. The relative movement between the chromophore and Asp-87 would therefore be smaller, and would yield a relatively stable electric field of amino acids, thereby proving the existence of stable optical properties of chromophores in these polypeptides. From this, we concluded that our results are valid, even without consideration of the chromophores in the simulation calculation. Future studies will attempt to include the chromophore in such calculations.

Effect of the vibrational state on biological functions

The vibrational state of the protein may play an important role in the mechanism of energy transfer within C-PC, and from C-PC to APC. When we calculated the normal mode of the C-PC subunit, only the dihedral angles were treated as independent variables, while bond lengths and bond angles were kept fixed. Furthermore, the vibrational frequencies were limited to the range from 1.7 cm^{-1} to 969 cm^{-1} in the

α-subunit and from 1.5 cm^{-1} to 1007 cm^{-1} in the β-subunit. These values corresponded to 30 fs to 20 ps in the time region for both subunits. Because the energy transfer time in the C-PC trimer is reportedly in the range of a few picoseconds (Gillbro et al., 1993) and that from C-PC to APC is $<\sim$40 ps (Mimuro et al., 1989), the value was about a thousand times the period of the fastest vibrational mode that we obtained in the present study. This might mean that the vibrations around dihedral angles are more important than any other vibrations when one considers the effect of the vibrational states for the energy transfer process from C-PC to APC. Further studies will explore such energy transfers in more detail.

The authors acknowledge Dr. K. Odai at the North Shore College and H. Fujisaki at the University of Tokyo for their help in making the graph of correlation coefficient maps in color.

This work was supported in part by financial aid from the Ministry of Education, Science, Sports, and Culture, Japan Grants 08309010, 10440240, and 11874119 (to M.M.) and 07280101 (to H.W.).

REFERENCES

Bald, D., J. Kruip, and M. Rögner. 1996. Supramolecular architecture of cyanobacterial thylakoid membranes: how is the phycobilisome connected with the photosystems? *Photosynth. Res.* 49:103–118.

Bernstein, F. C., T. F. Koetzle, G. J. B. Williams, E. F. Meyer, M. D. Brice, J. R. Rodgers, O. Kennard, T. Shimanouchi, and M. Tasumi. 1977. The Protein Data Bank: a computer-based archival file for macromolecular structures. *J. Mol. Biol.* 122:535–542.

Brejc, K., R. Ficner, R. Huber, and S. Steinbacher. 1995. Isolation, crystallization, crystal structure analysis and refinement of allophycocyanin from the cyanobacterium *Spirulina platensis* at 2.3 Å resolution. *J. Mol. Biol.* 249:424–440.

Bryant, D. A. 1991. Cell Culture and Somatic Cell Genetics of Plants, Vol. 7B (L. Bogorad and I. K. Vasil, editors). Academic Press, New York, London. 257–330.

Chang, W., T. Jiang, Z. Wan, J. Zhang, Z. Yang, and D. Liang. 1996. Crystal structure of R-phycoerythrin from *Polysiphonia urceolata* at 2.8 Å resolution. *J. Mol. Biol.* 262:721–731.

Dürring, M., R. Huber, W. Bode, R. Rümbeli, and H. Zuber. 1990. Refined three-dimensional structure of phycoerythrocyanin from the cyanobacterium *Mastigocladus laminosus* at 2.7 Å. *J. Mol. Biol.* 211:633–644.

Dürring, M., G. B. Schmidt, and R. Huber. 1991. Isolation, crystallization, crystal structure analysis and refinement of constitutive C-phycocyanin from the chromatically adapting cyanobacterium *Fremyella diplosiphon* at 1.66 Å resolution. *J. Mol. Biol.* 217:577–592.

Ficner, R., and R. Huber. 1993. Refined crystal structure of phycoerythrin from *Porphyridium cruentum* at 0.23 nm resolution and localization of the subunit. *Eur. J. Biochem.* 218:103–106.

Ficner, R., K. Lobeck, G. Schmidt, and R. Huber. 1992. Isolation, crystallization, crystal structure analysis and refinement of B-phycoerythrin from the red alga *Porphyridium sordidum* at 2.2 Å resolution. *J. Mol. Biol.* 228:935–950.

Gantt, E. 1981. Phycobilisomes. *Annu. Rev. Plant Physiol.* 32:327–347.

Gantt, E., and S. F. Conti. 1966. Granules associated with the chloroplast lamellae of *Porphyridium cruentum*. *J. Cell Biol.* 29:423–434.

Gillbro, T., A. V. Sharkov, I. V. Eryukov, E. V. Khoroshilov, P. G. Kryukov, R. Fisher, and H. Scheer. 1993. Förster energy transfer between neighboring chromophores in C-phycocyanin trimers. *Biochim. Biophys. Acta.* 1140:321–326.

Glazer, A. N. 1985. Light harvesting by phycobilisomes. *Annu. Rev. Biochem.* 14:47–77.

Glazer, A. N. 1989. Light guides. *J. Biol. Chem.* 264:1–4.

Go, M. 1981. Correlation of DNA exonic regions with protein structural units in hemoglobin. *Nature.* 291:90–92.

Go, M. 1983. Modular structural units, exons, and function in chicken lysozyme. *Proc. Natl. Acad. Sci. U.S.A.* 80:1964–1968.

Go, N., T. Noguti, and T. Nishikawa. 1983. Dynamics of a small globular protein in terms of low-frequency vibrational modes. *Proc. Natl. Acad. Sci. U.S.A.* 80:3696–3700.

Go, M., and M. Nosaka. 1987. Protein architecture and the origin of intron. *Cold Spring Harbor Symp. Quant. Biol*. 52:915–924.

Go, M., and T. Noguti. 1995. Putative origin of introns deduced from protein anatomy. *In* Tracing Biological Evolution in Protein and Gene Structures (M. Go and P. Schimmel, editors). Elsevier, Amsterdam. 229–235.

Grossman, A. R., M. R. Schaefer, G. G. Chiang, and J. L. Collier. 1993. The phycobilisome, a light-harvesting complex responsive to environmental conditions. *Microbiol. Rev.* 57:725–749.

Herzberg, O., C. C. H. Chen, G. Kapadia, M. McGuire, L. J. Carroll, S. J. Noh, and D. Dunaway-Mariano. 1996. Swiveling-domain mechanism for enzymatic phosphotransfer between remote reaction sites. *Proc. Natl. Acad. Sci. U.S.A.* 93:2652–2657.

Hoffman, E., P. Wrench, F. P. Sharples, R. Hiller, W. Welte, and K. Diederichs. 1996. Structural basis of light harvesting by carotenoids: peridinin-chlorophyll-protein from *Amphidinium carterae*. *Science.* 272: 1788–1791.

Jiang, T., J. Zhang, and D. Liang. 1999. Structure and function of chromophores in R-PE at 1.9 Å resolution. *Proteins: Struct., Funct., Genet.* 34:224–231.

Karrasch, S., P. A. Bullough, and R. Ghosh. 1995. The 8.5 Å projection map of the light-harvesting complex I from *Rhodospirillum rubrum* reveals a ring composed of 16 subunits. *Eur. Mol. Biol.* 14:631–638.

Kikuchi, H., T. Sugimoto, and M. Mimuro. 1997. An electronic state of the chromophore, phycocyanobilin, and its interaction with the protein moiety in C-phycocyanin: protonation of the chromophore. *Chem. Phys. Lett.* 274:460–465.

Koepke, J., X. Hu, C. Muenke, K. Schulten, and H. Michel. 1996. The crystal structure of the light-harvesting complex II (B800–850) from *Rhodospirillum molischianum*. *Structure.* 4:581–597.

Kraulis, P. 1991. MOLSCRIPT: a program to produce both detailed and schematic plots of protein structure. *J. Appl. Crystallogr.* 24:946–950.

Levitt, M., C. Sander, and P. S. Stern. 1985. Protein normal-mode dynamics: trypsin inhibitor, crambin, ribonuclease and lysozyme. *J. Mol. Biol.* 181:423–447.

McDermott, G., S. M. Prince, A. A. Freer, A. M. Hawthonthwaite-Lawless, M. Z. Rapiz, R. J. Cogdell, and N. W. Issacs. 1995. Crystal structure of an integral membrane light-harvesting complex from photosynthetic bacteria. *Nature.* 374:517–521.

Mimuro, M., H. Kikuchi, and A. Murakami. 1999. Concepts in Photobiology: Photosynthesis and Photomorphogenesis (G. S. Singhal, G. Renger, S. K. Sopory, K-D. Irrgang, and Govindjee, editors). Narosa Publishing House, New Delhi, India. 104–135.

Mimuro, M., I. Yamazaki, N. Tamai, and T. Kato. 1989. Excitation energy transfer in phycobilisomes at −196°C isolated from the cyanobacterium *Anabaena variabilis* (M-3): evidence for the plural transfer pathways to the terminal emitters. *Biochim. Biophys. Acta.* 973:153–162.

Momany, F. A., R. F. McGuire, A. W. Burgess, and H. A. Schraga. 1975. Energy parameters in polypeptides. VII. Geometric parameters, partial atomic charges, nonbonded interactions, hydrogen bond interactions, and intrinsic torsional potentials for the naturally occurring amino acids. *J. Phys. Chem.* 79:2361–2381.

Nemethy, G., M. S. Pottle, and H. A. Scheraga. 1983. Energy parameters in polypeptides. 9. Updating of geometrical parameters, nonbonded interactions, and hydrogen bond interactions for the naturally occurring amino acids. *J. Phys. Chem.* 87:1883–1887.

Nishikawa, T., and N. Go. 1987. Normal modes of vibration in bovine pancreatic trypsin inhibitor and its mechanical property. *Proteins.* 2:308–329.

Noguti, T., H. Sakakibara, and M. Go. 1993. Localization of hydrogen-bonds within modules in barnase. *Proteins.* 16:357–363.

Pariser, R., and R. G. Parr. 1953a. A semi-empirical theory of the electronic spectra and electronic structure of complex unsaturated molecules. I. *J. Chem. Phys.* 21:466–471.

Pariser, R., and R. G. Parr. 1953b. A semi-empirical theory of the electronic spectra and electronic structure of complex unsaturated molecules. II. *J. Chem. Phys.* 21:767–776.

Phillips, S. E. V. 1980. Structure and refinement of oxymyoglobin at 1.6 Å resolution. *J. Mol. Biol.* 142:531–554.

Pople, J. A. 1953. Electron interaction in unsaturated hydrocarbons. *Trans. Faraday Soc.* 49:1375–1385.

Reuter, W., G. Wiegand, R. Huber, and M. E. Than. 1999. Structural analysis at 2.2 Å of orthorhombic crystals presents the asymmetry of the allophycocyanin-linker complex, $AP{\cdot}L_C^{7,8}$, from phycobilisomes of *Mastigocladus laminosus*. *Proc. Natl. Acad. Sci. U.S.A.* 96:1363–1368.

Ritter, S., R. G. Hiller, P. M. Wrench, W. Welte, and K. Diederichs. 1999. Crystal structure of a phycourobilin-containing phycoerythrin at 1.90 Å resolution. *J. Struct. Biol.* 126:86–97.

Rüdiger, W. 1994. Progress in Phycological Research, Vol. 10 (F. E. Round and D. J. Chapman, editors). Biopress, Bristol, U.K.. 97–135.

Sakuranaga, M., K. Nakachi, and H. Suzuki. 1979. Theory of formamide and its related compound by INDO-CI method. *J. Phys. Soc. Jpn.* 46:944–951.

Sato, Y., Y. Niimura, K. Yura, and M. Go. 1999. Module-intron correlation and intron sliding in family F/10 xylanase genes. *Gene.* 238:93–101.

Scharnagl, C., and S. Schneider. 1989. UV-visible absorption and circular dichroism spectra of the subunits of C-phycocyanin. I. Quantitative assessment of the effect of chromophore-protein interaction in α-subunit. *J. Photochem. Photobiol. B: Biol.* 3:603–615.

Schirmer, T., W. Bode, R. Huber, W. Sidler, and H. Zuber. 1985. X-ray crystallographic structure of the light-harvesting biliprotein C-phycocyanin from the thermophilic cyanobacterium *Mastigocladus laminosus* and its resemblance to globin structures. *J. Mol. Biol.* 184: 257–277.

Schirmer, T., R. Huber, M. Schneider, W. Bode, M. Miller, and M. L. Hackert. 1986. Crystal structure analysis and refinement at 2.5 Å of hexametric C-phycocyanin from the cyanobacterium *Agmenellum quadruplicatum*. The molecular model and its implications for light-harvesting. *J. Mol. Biol*. 188:651–676.

Sidler, W. A. 1994. The Molecular Biology of Cyanobacteria (D. A. Bryant, editor). Kluwer Academic, The Netherlands. 139–216.

Tandeau de Marsac, N. 1991. Cell Culture and Somatic Cell Genetics of Plants, Vol. 7B. (L. Bogorad and I. K. Vasil, editors). Academic Press, New York, London. 417–446.

Tandeau de Marsac, N., and G. Choen-Bazire. 1977. Molecular composition of cyanobacterial phycobilisomes. *Proc. Natl. Acad. Sci. U.S.A.* 74:1635–1639.

Wako, H. 1989a. Dynamic structures of globular proteins with respect to correlative movements of residues calculated in the normal mode analysis. *J. Protein Chem.* 8:589–607.

Wako, H. 1989b. Inspection of three-dimensional structures of proteins with dynamical information from the normal mode analysis. *Protein Seq. Data Anal.* 2:175–180.

Wako, H., S. Endo, K. Nagayama, and N. Go. 1995. FEDER/2: program for static and dynamic conformational energy analysis of macromolecules in dihedral angle space. *Comp. Phys. Commun.* 91:233–251.

Wako, H., and N. Go. 1987. Algorithm for rapid calculation of Hessian of conformational energy function of proteins by supercomputer. *J. Comp. Chem.* 8:625–635.